probable for Antarctica at that time[22]. It is curious that the Oligocene hiatus is not found in the central Pacific. Post-Oligocene erosion is found in the Samoan gap. the bottom water conduit into the central Pacific[23]. Dissolution of great quantities of carbonate in the Indian Ocean and south-west Pacific in the Oligocene is possibly related to the contemporaneous high carbonate sedimentation elsewhere in the Pacific and Atlantic as the ocean responded to the need to maintain a chemical balance. Also, it is possible that at this time Ross Sea water was confined to the south-west Pacific by Melanesia and thus had relatively little influence in the regions farther north.

Between the late early Eocene and the middle of the Oligocene climatic conditions in Antarctica were probably a little warmer. This was sufficient to reduce the supply of Antarctic Bottom Water, encourage increased surface productivity, and diminish the intensity of current activity to the point where sedimentation could resume. The Oligocene hiatus was brought to a close by the gradual establishment. of the present pattern of circum-Antarctic flow sometime near the end of the Oligocene[24]. This again reduced the inhibiting influence of Antarctic Bottom Water on sedimentation in the ocean basins farther north, since a substantial proportion of the Antarctic Bottom Water was diverted into circumpolar flow and proportionately less found its way into the basins.

This attempt to attribute regional patterns of unconformities to climatic events in Antarctica is incomplete in several respects. First, the present day pattern of Antarctic Bottom Water circulation and its effects on deep ocean sedimentation are not entirely clear, much less these effects 60 Myr ago. Palaeo-bathymetry models would be helpful, as would further hydrographic stations and piston cores in the Indian Ocean. Second, present understanding of what effect Antarctic glaciation had on ocean surface water movements is equally vague. These currents have probably contributed to forming the hiatuses at shallow sites. We recommend experimental and analytical study of these currents taking into account continental dispersion and palaeowinds[25]. Finally, more precise evaluations of the stratigraphy at each site will result in a more refined picture of palaeocirculation patterns.

W. H. Berger, J. V. Gardner, T. C. Moore and E. L. Winterer reviewed the manuscript and made suggestions. The DSDP is supported by the National Science Foundation.

1. von der Borch, C. D., et al., *Init. Rep. Deep Sea Drilling Project*, 22 (US Government Printing Office, Washington, DC, 1974).
2. Whitmarsh, R. B., et al., *Init. Rep. Deep Sea Drilling Project*, 23 (US Government Printing Office, Washington, DC, 1974).
3. Fisher, R. L., et al., *Init. Rep. Deep Sea Drilling Project*, 24 (US Government Printing Office, Washington, DC, 1974).
4. Simpson, E. S. W., et al., *Init. Rep. Deep Sea Drilling Project*, 25 (US Government Printing Office, Washington, DC, 1974).
5. Davies. T. A., et al., *Init. Rep. Deep Sea Drilling Project*, 26 (US Government Printing Office, Washington, DC, in the press).
6. Heirtzler, J. R., et al., *Init. Rep. Deep Sea Drilling Project*, 27 (US Government Printing Office, Washington, DC, 1974).
7. Hayes, D. E., Frakes, L. A., Barrett, P., Burns, D. A., Chen, P., Ford, A. B., Kaneps, A. G., Kempe, E. M., McCollum, D. W., Piper, D. J. W., Wall, R. E., and Webb, P. N., *Geotimes*, 18 (6), 19-24 (1973).
8. Kennett, J. P., Burns, R. E., Andrews, J. E., Churkin, M., Davies, T. A., Dumitrica, P., Edwards, A. R., Galehouse, J. S., Packham, G. H., and van der Lingen, G. J., *Nature phys. Sci.*, 239, 51-55 (1972).
9. Brown, D. A., Campbell, K. S. W., and Crook, K. A. W., *The Geological Evolution of Australia and New Zealand* (Pergamon, London, 1968).
10. Davies, H. L., and Smith, I. E., *Bull. geol. Soc. Am.*, 82, 3299-3312 (1971).
11. Hornibrook, N. de B., *N.Z.J. Geol. Geophys.*, 9, 458-470 (1966).
12. Carter, R. M., and Landis, C. A., *Nature*, 237, 12-13 (1972).
13. Winterer, E. L., et al., *Init. Rep. Deep Sea Drilling Project*, 17 (US Government Printing Office, Washington, DC, 1973).
14. Tracey, J. I., et al., *Init. Rep. Deep Sea Drilling Project*, 8 (US Government Printing Office, Washington, DC, 1971).
15. Maxwell, A. E., von Herzen, R. P., Hsu, K. K., Andrews, J. E., Saito, T., Percival, S. F., Milow, E. D., Boyce, R. E., *Science*, 168, 1047-1058 (1970).
16. Douglas, R. G., Roth, P. H., and Moore, T. C., *Init. Rep. Deep Sea Drilling Project*, 17, 905-909 (US Government Printing Office, Washington, DC, 1973).
17. Luyendyk, B. P., and Davies, T. A., *Init. Rep. Deep Sea Drilling Project*, 26, 909-943 (US Government Printing Office, Washington, DC, in the press).
18. Kent, P. E., *Init. Rep. Deep Sea Drilling Project*, 25, 679-684 (US Government Printing Office, Washington, DC, 1974).
19. Berger, W. H., and Winterer, E. L., in *Pelagic Sediments on Land and in the Ocean* (edit. by Hsu, K. J., and Teulsyns, H.), (Zurich, in the press).
20. Heezen, B. C., and Hollister, C. D., *The Face of the Deep* (Oxford Univ. Press, New York, 1971).
21. Hayes, D. C., and Ringis, J., *Nature*, 243, 454-458 (1973).
22. Margolis, S. V., and Kennett, J. P., *Science*, 170, 1085-1087 (1970).
23. Hollister, C., Johnson, D. A., and Lonsdale, P., *J. Geol.*, 82, 275-300 (1974).
24. Kennett, J. P., Houtz, R. E., Andrews, P. B., Edwards, A. R., Gostin, V. A., Hajos, M., Hampton, M., Jenkins, D. G., Margolis, S. V., Ovenshine, A. T., and Perch-Nielsen, K., *Science*, 186, 144-147 (1974).
25. Luyendyk, B. P., Forsyth, D., and Phillips, J. D. *Bull. geol. Soc. Am.*, 83, 2649-2664 (1972).
26. McKenzie, D. P., and Sclater, J. G., *Geophys. J. R. astr. Soc.*, 25, 437-528 (1971).

Structure and assembly of filamentous bacterial viruses

D. A. Marvin & E. J. Wachtel

Department of Molecular Biophysics and Biochemistry, Yale University, New Haven, Connecticut 06520

The protein coat of filamentous bacterial viruses is constructed from segments of α helix that extend in an axial direction, and overlap each other like shingles or fish scales to form a hollow cylindrical shell. This hollow shell contains the viral DNA.

THE protein coat of filamentous bacterial viruses[1,2] is rich in α helix. This has enabled us to develop a model for the virus structure. We have used low resolution X-ray diffraction data to define the general arrangement of α helices, followed by molecular model building to define atomic positions. Our model has implications for the morphogenesis of these viruses, and also for the structure of linear assemblies of proteins in general.

Filamentous bacterial viruses consist of linear assemblies of coat protein subunits encapsulating single-stranded, circular DNA. The virions measure about 60 Å in diameter by 10,000 to 20,000 Å long, depending on the strain, and contain no more than 12% by weight of DNA. The major coat protein in all strains comprises about 99% of the viral protein, has a molecular weight of about 5,000, and is largely α helical. Their relative simplicity and the relatively high quality of their X-ray diffraction patterns makes these viruses uniquely valuable models for the study of the molecular structure of fibrous proteins and
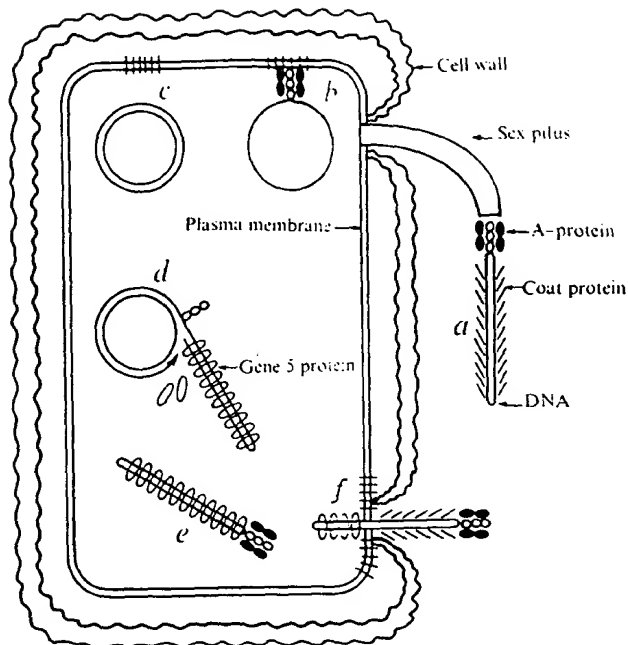
Fig. 1 Schematic illustration of some features of the filamentous bacterial virus life cycle. Successive stages are drawn counterclockwise around the bacterium, although it is unlikely that all stages would be found at once in any given bacterium. The entire illustration is consistent with current data, but some features are less solidly supported by experiment than others. *a*, The virus attaches to the Gram-negative bacterium by means of a minor coat protein, the A protein (the bacterial attachment site is the sex-pilus for some strains[2] but not others[28,29]) *b*. The viral DNA and A protein[30] enter the bacterium, leaving the major coat protein at the plasma membrane[27]. *c*, The viral DNA is converted to a duplex form, that replicates to give several hundred progeny duplexes. Viral DNA replication may require the presence of viral coat protein in the membrane[31], perhaps to create a new site for DNA replication[32]. *d*, The progeny duplex spins off a single-stranded tail that is coated with the protein product of viral gene 5. *e*, The DNA is closed to give a circular DNA molecule in a linear DNA-gene 5 protein complex[33]. *f*, The viral DNA passes out through the bacterial envelope. The gene 5 protein is displaced from the DNA by coat protein that had previously been deposited at the plasma membrane[25]. The completed virion is released from the bacterium without lysing or otherwise killing the bacterium[34]. Inhibition of viral assembly in contrast does kill the host in a process involving the gene 5 protein[35]. More complete citations of the earlier literature are given in ref. 2.

nucleoproteins. In addition, their unusual life cycle (Fig. 1) makes them interesting systems for the study of dynamic molecular interactions such as the displacement of one protein by another from a nucleoprotein complex, and the transport of macromolecules across membranes.

Structures of these viruses

Concentrated gels of filamentous bacterial virus can be oriented in fibres for X-ray diffraction studies[3]. Two classes of diffraction pattern, differing in detail, were found during a survey of various strains carried out in this laboratory[4,5]. The class I pattern is given by the fd, f1, M13, If1, and IKe strains[4]; the class II pattern is given by the Pf1 and Xf strains[5]. The class II pattern is simpler to interpret, and has therefore been analysed in more detail[5]. The position of diffracted intensity on the pattern indicates[6] that the protein subunits in the virus are arranged on a helix of pitch ~15 Å, with 4.4 subunits in one pitch length of the helix (Fig. 2). The relative magnitudes of diffracted intensity indicate that the diffracting material at each surface lattice point is elongated into a rod that makes an angle of about 20° with the helix axis, and also tilts from large to small radius in the virus. The orientation determined for the rods of electron density is such that rods originating on one turn of the helix inter-digitate between rods originating on the next turn.

Spectroscopic measurements[7,8] show that the α-helix content

of the coat protein approaches 100%. We have therefore assumed that the rods of electron density found from qualitative analysis of the X-ray pattern can be considered as single rods of α-helical protein measuring 10 Å by 70 Å, the dimensions of an α helix with molecular weight 5,000, and have used model-building techniques for further analysis of the structure. The α helix was represented in initial models by a row of points distributed on a curve 70 Å long. The Fourier transform[6] of this repeat unit in the virus helix was calculated for various orientations and curvatures of the row, and compared with the class II diffraction pattern. The results of many trial calculations confirmed the conclusions about orientation of rods of electron density that were derived from direct analysis of the diffraction pattern. For the next stage in our model building, the row of points was replaced by a 70 Å polyalanine α helix. We generated the co-ordinates of atoms in this α helix by extending Crick's equation for the coordinates of a coiled coil[9] to allow for a change in radius of the α helix in the major helix frame. Scattering factors of atoms were modified as described by Wilkins and coworkers[10] to take into account the background electron density due to water and low density protein sidechains[11]. The contribution of the DNA to the calculated diffraction was ignored at this stage.

Both intrachain and interchain stereochemistry were included as further constraints on the model. The intrachain stereochemistry of the α-helix rod was refined by fitting a stereochemically perfect polypeptide chain to the rough guide coordinates generated for the curved α helix, using the computer program developed by Diamond[12]. The Ramachandran angles were $110° < \varphi < 133°$ and $123° < \psi < 149°$ over the length of the refined α helix, and internal hydrogen bond lengths of the refined structure were also within the permissible range for α helix[13]. The interchain stereochemistry (the distance between
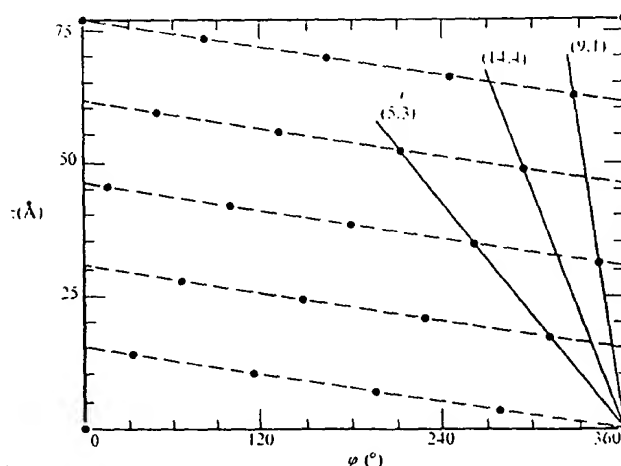

Fig. 2 Surface lattice of the class II helix. The lattice shows the 22 equivalent points in a 77 Å section of the virus helix, projected on to a cylindrical surface coaxial with the virus, which is then opened out flat and viewed from the outside of the helix. The dashed line shows the ~15 Å pitch of the virus helix. There are 22 units in 5 turns or 4.4 units per turn[5]. These helix parameters define the order of the Bessel functions predicted on each layer line of the helix diffraction pattern. In particular, for layer lines $l = 1, 2$ and 3, the lowest order Bessel functions are those with order $|n| = 9$, 4 and 5, respectively. The sign associated with $|n| = 5$ and 9 is opposite to that associated with $|n| = 4$. The sense of the helices with (n, l) indices (5, 3) and (9, 1) must be the same as that of the ~15 Å virus helix (they are shown as left-handed in this figure), but the absolute sense is not defined by the X-ray data. The fact that intensity is stronger on $l = 1$ and 3 than on $l = 2$ indicates that rods of electron density have the same sense as the ~15 Å helix. These rods of electron density roughly follow the $(\bar{1}4, 4)$ helix. The maxima of intensity on both $l = 1$ and $l = 3$ are observed at 0.1 Å^{-1} along the layer lines, even though the predicted Bessel function orders are quite different for these two layer lines. This indicates that the rods of electron density tilt from large to small radius as well as slewing around the virus[6].
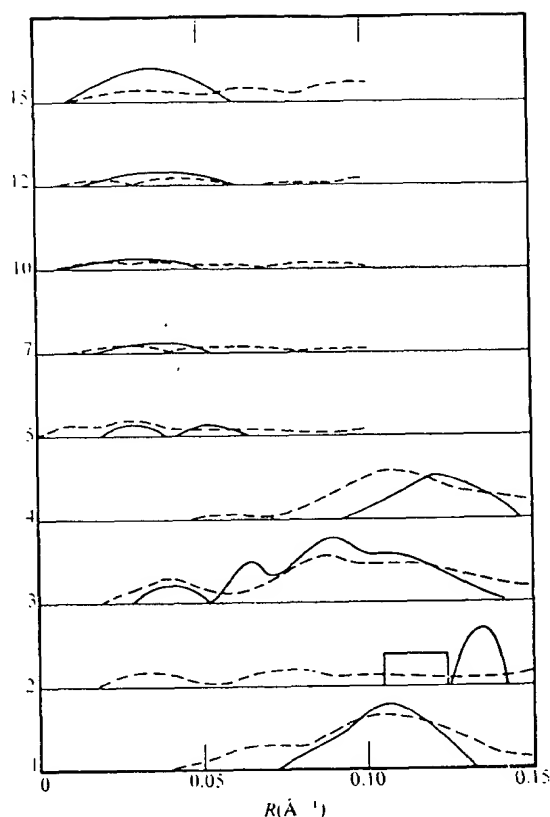
Fig. 3 Comparison of the calculated Fourier transform of the class II protein model with the observed diffraction amplitudes. Continuous diffraction on non-equatorial layer lines was measured[13-15] on a diffraction pattern of Pf1 taken at 98% relative humidity by Dr R. L. Wiseman[5] (film No. 2036). The cylindrically averaged Fourier transform was calculated for a *repeat* unit consisting of a 46-residue stretch of polyalanine α helix the axis of which roughly follows a segment of a conchospiral with α = −21° and γ = 11.5° between 14 Å and 26 Å radius. This repeat unit was placed in a left-handed helix having 22 units in 5 turns in an axial repeat *c* = 77 Å. Over most of the region of close contact between neighbouring α helices, distances between the α-helix axes were 10±1 Å and crossing angles between the axes were 9–12°. Observed amplitudes are solid lines; calculated amplitudes are dashed lines. The rectangular box on *l* = 2 represents integrated intensity for which the shape could not be determined. Analysis of the equator is discussed in ref. 15.

neighbouring α helices and the angle at which the axes of neighbouring helices cross each other) was such that sidechains on one α helix could fit into the space between sidechains on its neighbours in knobs-into-holes packing[9]. Only α helices whose axes follow a left-handed helical path can form satisfactory knobs-into-holes packing, indicating that the sense of the ∼15 Å virus helix is also left-handed (Fig. 2).

The resolution of the X-ray data is not sufficient to define the positions of specific sidechains, but reasonable assumptions about the orientation of the protein molecule can be made on general chemical grounds. The acidic N-terminal end of the Pf1 protein was placed at the outer radius of the virus, and the basic C-terminal end at the inner radius, as first suggested for fd[7]. The α helix was then rotated about its own axis so that arginine-44 and lysine-45 were directed inwards, towards the virus core; the acidic residues were directed outwards at the virus surface; and most of the hydrophobic residues were involved in contacts with neighbours[14].

There are narrow limits on the range of models that are consistent with all these stereochemical constraints and yet give calculated transforms similar to the observed. The observed and calculated transforms for the current best model are compared in Fig. 3. The model is illustrated in Figs 4 and 5.

Fourier analysis of the equatorial intensity (which gives information about the electron density projected down the long

axis of the virion) shows that the DNA occupies a central core surrounded by a shell of protein, with virtually no interpenetration of DNA and protein[15]. X-ray diffraction and chemical evidence. however. are insufficient for a detailed model of the DNA to be built at this time.

Symmetry and perturbation

An overlapping or shingled arrangement of axially elongated protein subunits as found for filamentous bacterial viruses is a stable and durable design for fibrous proteins. Larger bonding surfaces are available for interaction of subunits than would be available in a comparable structure made of globular subunits. In the minimum energy configuration[16] for such an assembly, there are likely to be regular contacts along the length of neighbouring subunits, resulting in similar bonds at different radii. These bonds will be related by symmetry elements that operate not just in the surface lattice of the helix, but in three dimensions.

For the conformation derived experimentally for class II coat protein subunits, the α-helix axis roughly follows a segment of a conchospiral, a space curve with many interesting symmetry properties[17,18]. The conchospiral is given by the equations

$$r = a\exp(\varphi \cot \alpha \sin \gamma)$$
$$z = c\exp(\varphi \cot \alpha \sin \gamma)$$
$$\tan \gamma = a/c,$$

where r, φ, z are cylindrical polar coordinates, α is the constant angle that the tangent to the curve makes with the z axis, and γ is the half-angle of the cone on which the conchospiral lies. This curve is the most symmetrical space curve aside from the circular helix. The curvature and torsion of the curve change continuously in a regular way as one progresses along the curve, giving regular internal symmetry. The segments of conchospiral in the filamentous virus helix are located so that each segment is roughly centred along its length between its nearest neighbours. There are two main kinds of intermolecular contacts: from any protein molecule to the proteins originating five and nine units, respectively, down the ∼15 Å virus helix (Fig. 5). In the class II structure these contacts are sufficiently similar so that each protein in the helix has essentially equivalent environments in both directions, although a faint meridional reflection on the ∼15 Å layer line indicates a slight perturbation repeating periodically about once per turn of the ∼15 Å virus helix. The corresponding meridional reflection on class I patterns, and by implication the associated perturbation, is much stronger[4]. Contacts between the class I α helices that correspond to the 0 to −5 class II contacts in Fig. 5 are regular, but contacts corresponding to 0 to −9 are irregular, with a perturbation that repeats about every five units. This perturbed configuration presumably optimises local contacts and is therefore more stable than any unperturbed configuration that could be formed by the class I subunits.

Three principles for the design of linear assemblies of proteins are suggested by the detailed studies of filamentous viruses. (1) Linear assemblies will often be composed of axially elongated overlapping subunits. (2) Interdigitation of elongated subunits in neighbouring turns of the helical array will be facilitated if there are (roughly) an odd number of units in two turns of the helix. (3) Contacts between interdigitating neighbours will often be improved by a perturbation away from the ideal helical positions, repeating once every turn of the helix, and giving rise to a set of meridional reflections at orders of a periodicity that corresponds to the pitch of the helix rather than to the subunit spacing. Overlapping arrangements of elongated subunits have been proposed for myosin filaments in muscle[19-21]. Sharp meridional reflections have been observed on diffraction patterns of many fibrous proteins[13], and in some cases have been interpreted in terms f perturbation. Som linear assemblies,
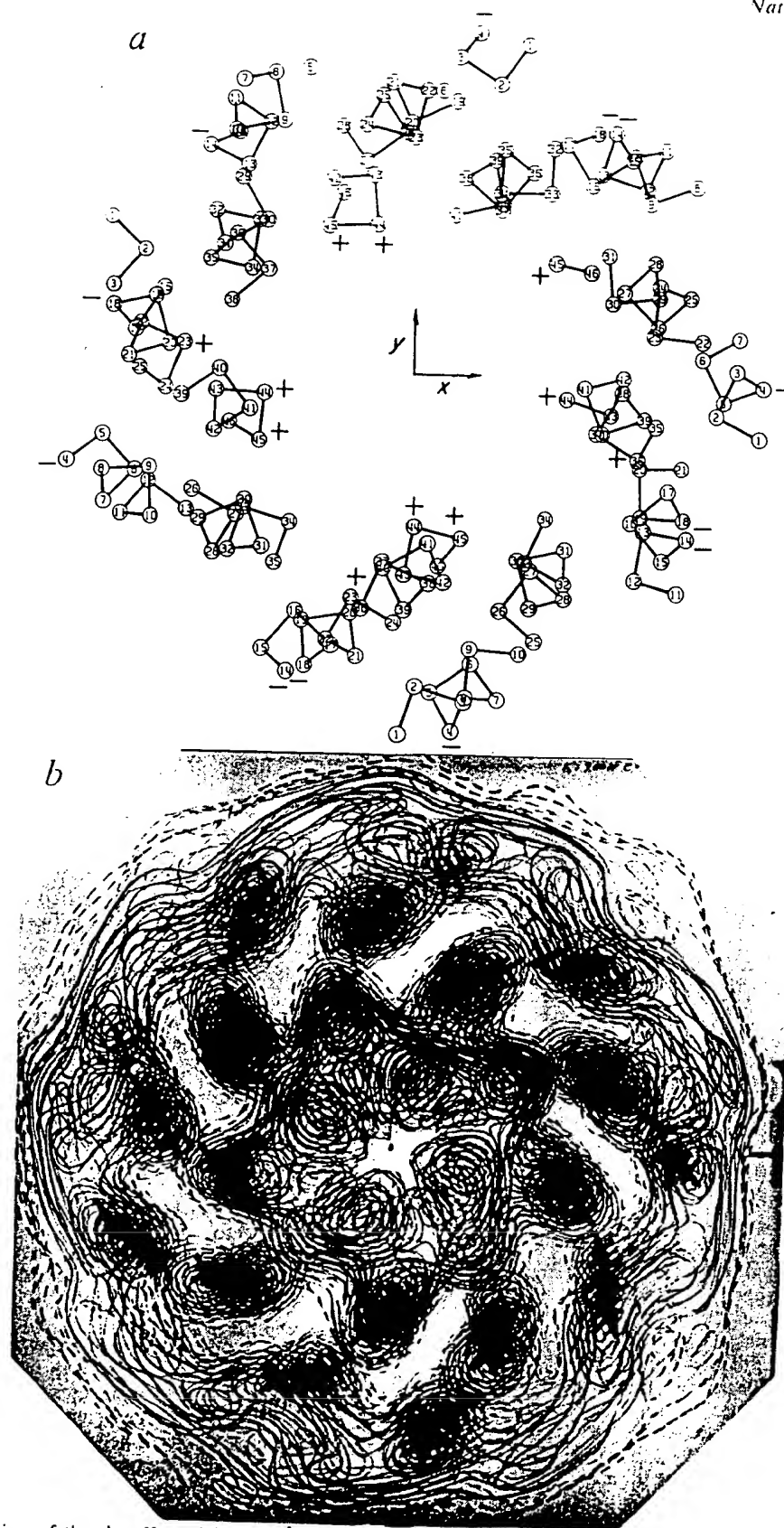
Fig. 4 Axial section of the class II model. A 14 Å slab through one virion, equivalent to four helix asymmetric units, is shown for convenience in visualising the packing of neighbours. *a*, Ball-and-stick representation of the α-carbon atoms, projected on to a plane normal to the axis of the virion. Numbers indicate residues. Several segments of different α helices overlap, but can be distinguished by discontinuities in the sequence of numbers. The basic residues (20, 44 and 45) and acidic residues (4, 14 and 18) are indicated by + and −, respectively. The box measures 30 Å on a side. *b*, Electron density in a corresponding slab, calculated[6] using[24] the observed amplitudes and the phases of the protein model shown in Fig. 3. For the equator, phases were taken from Fig. 7*b* of ref. 15, and amplitudes from continuous transform of a non-crystalline Pf1 fibre at 100% relative humidity, measured and corrected for residual crystalline reflections as described in ref. 15. Crosses indicate the positions of axes of α helices in the model. Zero contours are dashed and may enclose negative density. Although DNA was not included in the phasing, it is expected that phases calculated on the basis of the protein model alone will be approximately correct, and may reveal structure not included in the model, such as possible phosphate peaks in the central DNA region.
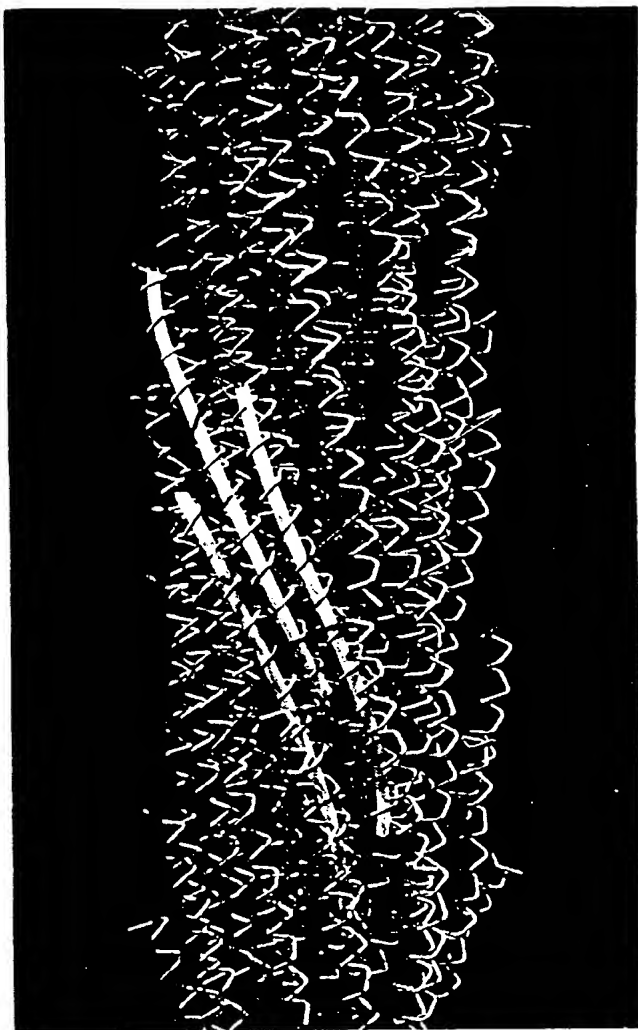
would leave the lipid off the water, taking associated DNA with it. The process would be akin to crystal growth where the growing point of the crystal is fixed in space so that the crystal must move away from the growing point. The sense of the process (the virion moves out of rather than into the bacterium) would depend on the details of the configurational change in the coat protein upon assembly. A similar process in reverse could drive the dissolution of protein off the virion into the lipid bilayer[25] and advance the DNA into the bacterium during infection. This model—that assembly of hydrophobic proteins within a lipid bilayer causes changes in the properties of the completed assembly so that it becomes more soluble than the monomer in an aqueous phase and thus moves out of the bilayer—could apply in general to transport of oligomeric or polymeric proteins through membranes.

This investigation was supported by a grant from the National Institutes of Health.

Fig. 5 Model of a 154 Å slab of the protein coat of the virus. The long axis of the virion is vertical. The protein subunits are represented by bent rod following the path from one α carbon to the next. Three neighbouring α helices are picked out by lengths of tubing; they are shown in the same view as Fig. 3 of ref. 14. The right-most α helix originates five units down the ∼ 15 Å helix with respect to the central α helix, and the left-most α helix originates nine units down. Note the gentle curve of the α helices, and the interdigitation of neighbouring helices. DNA would occupy the central cylindrical cavity in the protein shell. The outer diameter of the lucite support rod is 6 Å in the model.

such as microtubules or bacterial flagella that have been assumed to be composed of globular subunits[22-24] should perhaps be re-examined in the light of these principles.

Assembly

With the molecular structure of the virion in hand, we can discuss specific hypotheses about viral assembly. We assume the model of assembly illustrated in Fig. 1, and restrict ourselves to the steady-stage of assembly, after the forward end of the virion has passed across the membrane. The viral coat protein is a single rod of α helix with a hydrophobic central portion and hydrophilic ends. The protein could be excreted directly into the lipid bilayer[25] during synthesis[26], with its N-terminal end outwards and its long axis normal to the plane of the bilayer[2]. The DNA, stripped of the gene 5 protein would, form a condensation centre for the coat protein previously stored in the bilayer. As the protein assembled on to the DNA, its hydrophobic areas would become masked, so that the protein would become less soluble in lipid than in water and therefore

[1] Marvin, D. A., and Hoffmann-Berling, H., *Nature*, **197**, 517–518 (1963).
[2] Marvin, D. A., and Hohn, B., *Bact. Rev.*, **33**, 172–209 (1969).
[3] Marvin, D. A., *J. molec. Biol.*, **15**, 8–17 (1966).
[4] Marvin, D. A., Pigram, W. J., Wiseman, R. L., Wachtel, E. J., and Marvin, F. J., *J. molec. Biol.* **88**, 581–598 (1974).
[5] Marvin, D. A., Wiseman, R. L., and Wachtel, E. J., *J. molec. Biol.*, **82**, 121–138 (1974).
[6] Klug, A., Crick, F. H. C., and Wyckoff, H. W., *Acta Cryst.*, **11**, 199–213 (1958).
[7] Asbeck, F., Beyreuther, K., Köhler, H., von Wettstein, G., and Braunitzer, G., *Hoppe-Seyler's Z. physiol. Chem.*, **350**, 1047–1066 (1969).
[8] Day, L. A., *J. molec. Biol.*, **15**, 395–398 (1966); **39**, 265–277 (1969).
[9] Crick, F. H. C., *Acta Cryst.*, **6**, 685–689; 689–697 (1953).
[10] Langridge, R., Marvin, D. A., Seeds, W. E., Wilson, H. R., Hooper, C. W., Wilkins, M. H. F., and Hamilton, L. D., *J. molec. Biol.*, **2**, 38–64 (1960).
[11] Fraser, R. D. B., MacRae, T. P., and Miller, A., *J. molec. Biol.*, **14**, 432–442 (1965).
[12] Diamond, R., *Acta Cryst.*, **21**, 253–266 (1966).
[13] Fraser, R. D. B., and MacRae, T. P., *Conformation in fibrous proteins* (Academic Press, New York, 1973).
[14] Nakashima, Y., Wiseman, R. L., Konigsberg, W., and Marvin, D. A., *Nature*, **253**, 68–71 (1975).
[15] Wachtel, E. J., Wiseman, R. L., Pigram, W. J., Marvin, D. A., and Manuelidis, L., *J. molec. Biol.*, **88**, 601–618 (1974).
[16] Caspar, D. L. D., and Klug, A., *Cold Spring Harb. Symp. quant. Biol.*, **27**, 1–24 (1962).
[17] Thompson, D. W., *On growth and form* (Cambridge University Press, Cambridge, 1942).
[18] Coxeter, H. S. M., *Introduction to geometry* (Wiley, New York, 1969).
[19] Young, M., King, M. V., O'Hara, D. S., and Molberg, P. J., *Cold Spring Harb. Symp. quant. Biol.*, **37**, 65–76 (1972).
[20] Pepe, F. A., *Cold Spring Harb. Symp. quant. Biol.*, **37**, 97–108 (1972).
[21] Squire, J. M., *J. molec. Biol.*, **77**, 291–323 (1973).
[22] Lowy, J., and Hanson, J., *J. molec. Biol.*, **11**, 293–313 (1965).
[23] Olmsted, J. B., and Borisy, G. G., *A. Rev. Biochem.*, **42**, 507–540 (1973).
[24] Erickson, R. O., *Science*, **181**, 705–716 (1973).
[25] Smilowitz, H., Carson, J., and Robbins, P. W., *J. supramolec. Struct.*, **1**, 8–18 (1972).
[26] Costerton, J. W., Ingram, J. M., and Cheng, K.-J., *Bact. Rev.*, **28**, 87–110 (1974).
[27] Smilowitz, H., *J. Virol.*, **13**, 94–99 (1974).
[28] Brodt, P., Leggett, F., and Iyer, R., *Nature*, **249**, 856–858 (1974).
[29] Bradley, D. E., *Biochem. biophys. Res. Commun.*, **57**, 893–900 (1974).
[30] Jazwinski, S. M., Marco, R., and Kornberg, A., *Proc. natn. Acad. Sci. U.S.A.*, **70**, 205–209 (1973).
[31] Timmis, K., Early, P. W., and Marvin, D. A., *Biochem. biophys. Res. Commun.*, **57**, 263–270 (1974).
[32] Marvin, D. A., *Nature*, **219**, 485–486 (1968).
[33] Pratt, D., Laws, P., and Griffith, J., *J. molec. Biol.*, **82**, 425–439 (1974).
[34] Hoffmann-Berling, H., and Mazé, R., *Virology*, **22**, 305–313 (1964).
[35] Timmis, K., and Marvin, D. A., *Virology*, **59**, 293–300 (1974).
[36] Marvin, D. A., Wilkins, M. H. F., and Hamilton, L. D., *Acta Cryst.*, **20**, 663–669 (1966).